



Original article

Synthesis of TiO₂ nanoparticles by electrochemical method and their antibacterial application

Priyanka Anandgaonker, Ganesh Kulkarni, Suresh Gaikwad, Anjali Rajbhoj  [Show more](#)  Outline |  Share  Cite<https://doi.org/10.1016/j.arabjc.2014.12.015> [Get rights and content](#) Under a Creative Commons [license](#) 

open access

Abstract

Titanium dioxide nanoparticles were successfully prepared by electrochemical method. The tetra propyl ammonium bromide salt was used as stabilizing agent in an organic medium *viz.* tetra hydro furan (THF) and acetonitrile (ACN) in 4:1 ratio by optimizing current density. The parameters such as current density, solvent polarity, distance between electrodes and concentration of stabilizers were used to control the size of nanoparticles. The synthesized titanium dioxide nanoparticles were characterized by using UV–Visible spectroscopy, X-ray diffraction, scanning electron microscopy (SEM), energy dispersive spectrophotometer (EDS) and transmission electron microscopy (TEM) analysis techniques. TEM analysis proved a nearly tetragonal structure with size of 25–30nm which was in agreement with the result calculated from the XRD analysis. EDS analysis revealed the presence of Ti and O element. The nanoparticles were screened for their *in vitro* antibacterial activity against human pathogens such as gram negative *Escherichia coli* (*E. coli*), and gram positive *Staphylococcus aureus* strains and which proved excellent results.



Keywords

Titania nanoparticles; Tetra propyl ammonium bromide salt; Electrochemical reduction method; Human pathogens; Antimicrobial activity

1. Introduction

Nanomaterials, especially metal nanoparticles, have received much attention over the past decades because of their many technological applications that they have to offer (Cheng et al., 2012, Porod et al., 2003, Rothenberg et al., 2002, Cooper et al., 2014). Studying these applications has always been of great interest to many scientists. In fact, nanoparticles display completely unique properties in comparison with their bulk size counterparts. Nanoparticles are currently known as antibacterial materials. The antibacterial effect of metal nanoparticles has been attributed to their small size and high surface to volume ratio, which allows them to attach closely with microbial membranes and is not merely due to the release of metal ions in solution (Chwalibog et al., 2012). Among the inorganic antibacterial agents, metals and photocatalysts are most commonly used. Most metallic ions exhibit antimicrobial effect. For efficiency and safety reason, silver, copper and zinc are the most widely available metallic antibacterial agents (Gajbhiye et al., 2009, Akhavan, 2009, Xie et al., 2011).

TiO₂ nanoparticles, approximately less than 100nm in diameter, have become a new generation of advanced materials and are of great interest due to its different environmental applications, such as gas sensor (Obida et al., 2005, Tian et al., 2013) photocatalytic degradation of various contaminants in waste water treatment (Chong et al., 2010), degradation of carcinogenic dyes (Bumajdad et al., 2014), solar cell (Baraton, 2011). TiO₂ nanoparticles are used in cosmetics and filters that exhibit strong germicidal properties and remove odors. The TiO₂ photocatalysts have been investigated extensively for the killing or growth inhibition of bacteria due to its powerful oxidation strength, good chemical stability and nontoxicity (Kim et al., 2003, Liou and Chang, 2012, Foster et al., 2011). Being strong oxidant, the reactive oxygen species generated by the TiO₂ photocatalytic reactions cause various damages to microorganisms ensuring their rapid inactivation.

Generally, the most common approach in the literature for synthesizing and stabilizing TiO₂ nanoparticles is sol–gel method based on the hydrolysis of titanium alkoxide.

However, this method encounters some problem, such as weak anatase crystallinity and poor monodispersity. Therefore this study was designed to synthesize pure anatase TiO₂ nanoparticles by electrochemical method; a controlled current electrolysis is used throughout the synthesis process. The tetra propyl ammonium bromide salt used was highly soluble and dissociated in the solvent to play the role of electrolyte. It was absorbed on the metal oxide surface to stabilize the synthesized nanoparticles. The effect of change in current density on particle size was also studied. A bioevaluation assay of the inhibitory activity of the synthesized TiO₂ nanoparticles on bacterial strain was performed to establish the potential of these nanoparticles as antibacterial agents at different concentrations with well known antibiotics like Gentamicin.

2. Experimental methods

2.1. Materials

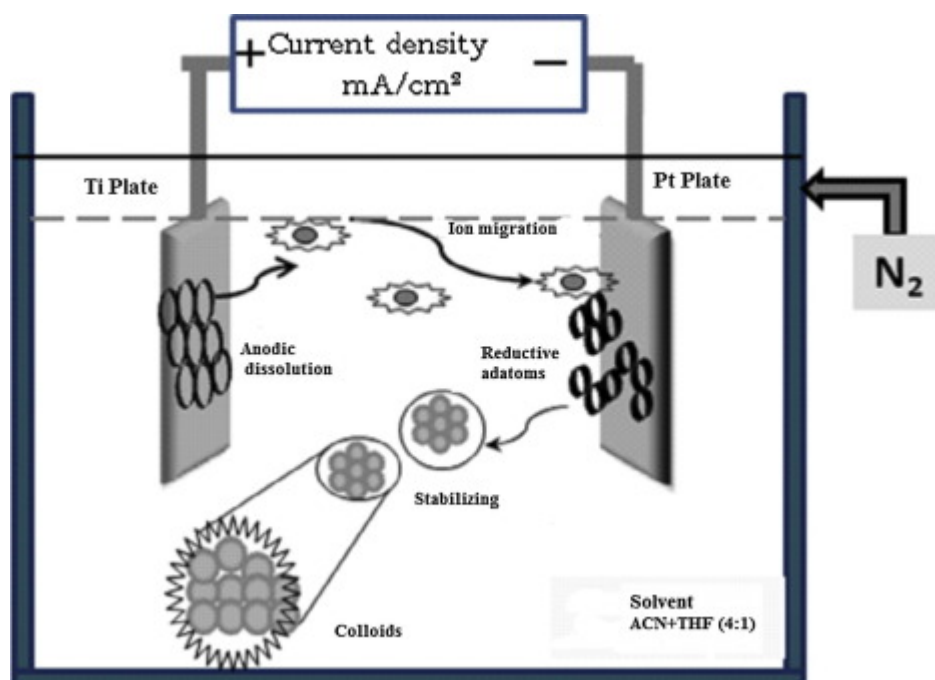
All chemicals (up to 98.99% purity) were purchased from Aldrich and Rankem chemical suppliers and used as received. *Staphylococcus aureus* (ATCC No. 25923) and *Escherichia coli* (ATCC No. 25922), provided by Govt. Institute of Science, Aurangabad 431,004. Antibiotics Gentamicin was subjected to analysis. Agar medium was used for screening the antibacterial activity.

2.1.1. Synthesis of titanium dioxide nanoparticles

The synthesis of titanium dioxide nanoparticles was done by electrochemical method (Reetz and Helbig, 1994, Reetz et al., 1995), for narrow size distributed metal nanoparticles. In the overall process the bulk metal is oxidized at the anode, the metal cations migrate to the cathode and reduction takes place with formation of metal or metal oxide in the zero oxidation state. Agglomeration with formation of undesired metal powder is prevented by the presence of the ammonium stabilizer.

As shown in Fig 1, in the initial experiment we have used a Titanium metal sheet (1×1 cm) as anode and a platinum sheet (1×1 cm) as the cathode. The two electrodes were 1 cm apart. Tetra Propyl Ammonium Bromide (TPAB-0.01 M) in acetonitrile/tetrahydrofuran (4:1) served as the supporting electrolyte. Upon applying current density we obtained >95% of titanium dioxide clusters stabilized by tetra propyl ammonium bromide (TPAB). Electrolysis was carried out in nitrogen atmosphere. Titanium dioxide nanoparticles were found to be white in color. Since the material was insoluble in the solvent mixture used, the work up turned out to be simple decantation, decanted solid product was washed with dry THF for three to four times to remove excess TPAB and dried under vacuum desiccators. This dried sample was calcinated at 550°C and stored in closed glass vials under ambient conditions. In order to study the

effect of current density on particle size, the current in the electrolysis process was varied from at 10mA/cm² to 14mA/cm². It was found that variation in current density affects the particle size of nanocluster in the electrolysis process.



[Download : Download high-res image \(154KB\)](#)

[Download : Download full-size image](#)

Figure 1. Diagram representing the synthesis process of TiO₂ nanoparticles.

Reaction mechanism for electrochemical synthesis of metal clusters:



[Download : Download high-res image \(51KB\)](#)

[Download : Download full-size image](#)

2.1.2. Characterization of titanium dioxide nanoparticles

The prepared titanium dioxide nanoparticles were characterized by UV–Visible spectrophotometry, XRD, TEM, SEM–EDS techniques. The wavelength of absorbance was determined by UV–Visible spectrophotometer [JASCO 503] using a quartz cuvette and acetonitrile/tetrahydrofuran as reference. The X-ray powder diffraction patterns of the TiO₂ nanoparticles were recorded on Bruker 8D advance X-ray diffractometer using Cu K α radiation of wavelength=1.54056Å. To study the morphology of TiO₂ nanoparticles, the SEM analysis was carried out with JEOL; JSM-6330 LA operated at 20.0kV and

1.0000nA. The presence and elemental composition in TiO₂ nanoparticles were examined using energy dispersive spectrophotometer (EDS). The TEM analysis was carried out with Philips model CM200 operated at 20–200kV.

2.1.3. Antibacterial activity experiment

Antibacterial activity of the TiO₂ nanoparticles was determined, using the agar well diffusion assay method (Thornberry, 1950). Approximately, 25 ml of molten and cooled nutrient agar media were poured in the sterilized petri dishes. The plates were left over night at room temperature to check for any contamination to appear. The bacterial test organism *S. aureus* and *E. coli* were grown in nutrient broth for 24h. A 100µl nutrient broth culture of each bacterial organism was used to prepare bacterial lawns. Agar wells were prepared with the help of a sterilized stainless steel cork borer. The wells in each plate were loaded with 100µl of different concentration of TiO₂ nanoparticles. Antibiotic gentamicin used as positive control for each bacterium to compare the inhibition of growth of bacteria with TiO₂ nanoparticles. The plates containing the bacteria and solutions of TiO₂ nanoparticles were incubated at 37°C. All the tests were repeated in triplicates. The antibacterial activity was taken on the basis of diameter of Zone of Inhibition which was measured at cross-angles after 24h of incubation and the mean of three readings is shown in Table 1. The inhibition of the bacterial growth on the agar plates by using different concentration of TiO₂ nanoparticles synthesized at two different current densities is shown in Fig. 6.

Table 1. In vitro antibacterial screening of synthesized titanium dioxide nanoparticles.

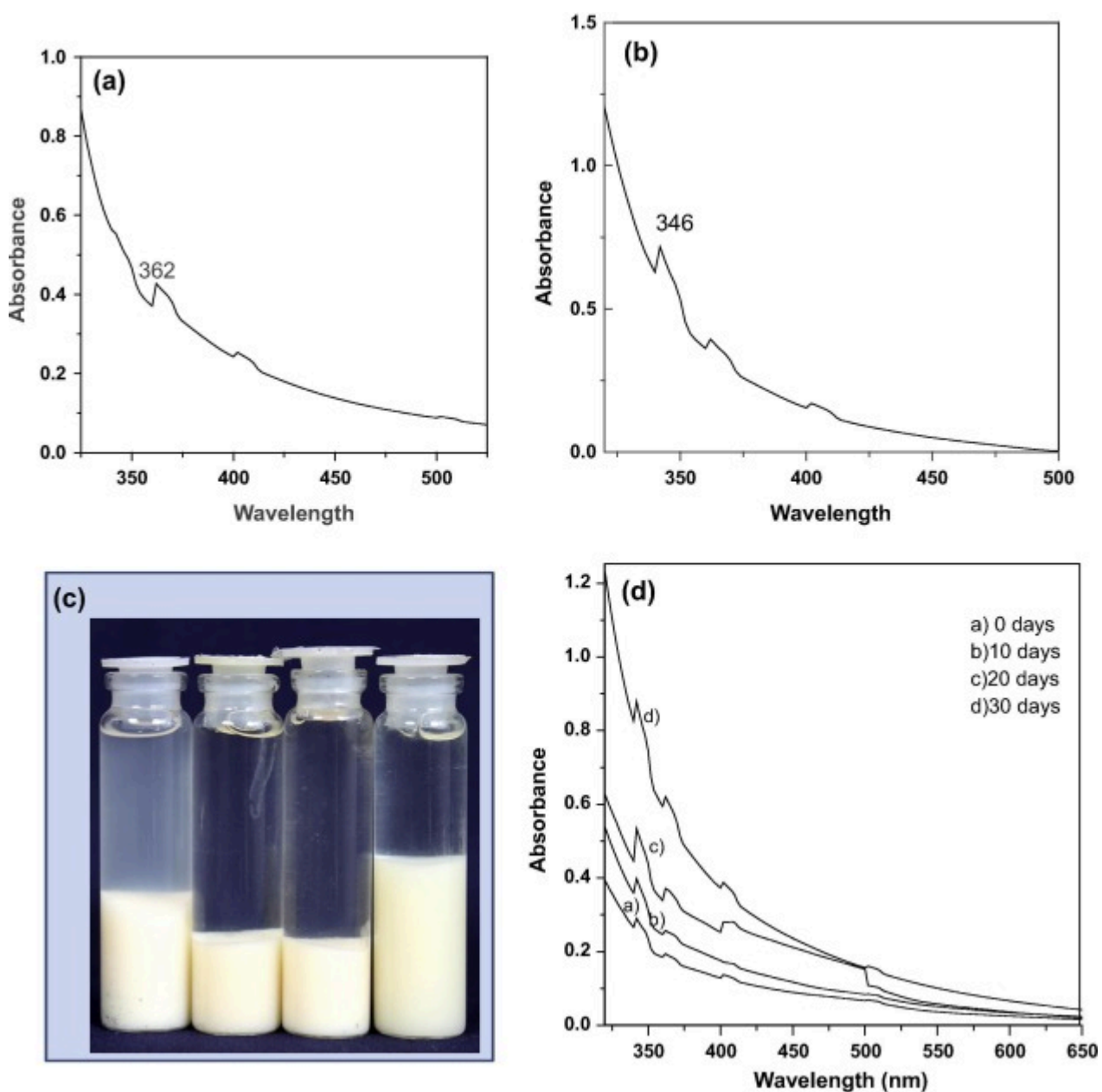
Human pathogenic bacteria	TiO ₂ nanoparticles				ACN+THF (4:1)		Gentamicin	
	10mA/cm ²		14mA/cm ²		50µl	100µl	50µl	100µl
	50µl	100µl	50µl	100µl				
<i>Zone of inhibition (mm)</i>								
<i>Staphylococcus aureus</i>	13.2	17.2	16.0	19.1	00	00	21.3	24.4
<i>E. coli</i>	10.5	14.3	15.2	17.0	00	00	19.2	22.8

3. Results and discussion

3.1. UV–Visible spectrophotometry

As the phenomenon of Surface Plasmon occurs only in the case of nanoparticles and not in case of bulk metallic particles, hence unique optical properties of nanoparticles can be

studied using UV–Visible spectroscopy (Burda et al., 2000). In present synthesis method as the electrochemical reduction proceeds, the color of reaction mixture changes from white to opaque milky white indicating formation of TiO₂ nanoparticles. About 4ml of colloidal reaction mixture was withdrawn after 2h to record UV–Visible spectrum. Prepared sample of TiO₂ was capped with TPAB at current densities 10mA/cm² and 14mA/cm² showed sharp peaks at 362nm and 346nm respectively indicating the formation of anatase TiO₂ in nanoform (Fig. 2a and b). The size and shape of nanoparticles could be qualitatively described by the peak position and shape of the absorption spectrum. General trend is that the absorption at long wavelengths was due to the scattering of light by big particles (Bian et al., 2008).



[Download : Download high-res image \(414KB\)](#)

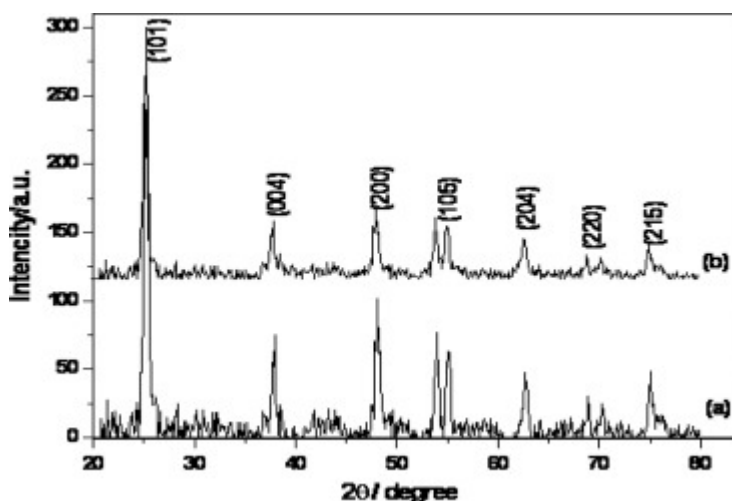
[Download : Download full-size image](#)

Figure 2. UV–Visible Spectra of TiO₂ nanoparticles synthesized at different current densities (a) at 10mA/cm² and (b) at 14mA/cm². (c) Shows photograph of colloidal TiO₂ nanoparticles stored in glass bottles. (d) Time dependence of the absorption spectrum of a TiO₂ nanoparticles colloid.

In the electrochemical method for the preparation of the metal nanoparticles, the size of the nanoparticles decreased with the increase in the current density. It can thus be said that the colloidal TiO₂ nanoparticles prepared at a current density of 10mA/cm² were bigger in size as compared to the colloidal TiO₂ nanoparticles prepared at a current density of 14mA/cm². As an evident from (Fig. 2d) the particles showed hardly any change in the absorption spectra even after a month of aging time, consistent with the highly stable nature of nanoparticles.

3.2. X-ray diffraction

The particle size of nanomaterials is related to the diffraction peak broadening, so X-ray diffraction spectra of synthesised TiO₂ nanoparticles were taken and particle size and phase composition were determined. Fig. 3 shows XRD pattern for TiO₂ nanoparticles. The lattice parameter observed $a=b=3.780$, $c=9.513$. The nanocrystalline anatase structure was confirmed by sharp peaks obtained corresponding to the planes (101), (004), (200), (105) (204), (220) and (215) indicates the tetragonal structure of TiO₂ nanoparticles. All peaks obtained were in good agreement with the JCPDS card no. 21-1272.



[Download : Download high-res image \(133KB\)](#)

[Download : Download full-size image](#)

Figure 3. XRD pattern of TiO₂ nanoparticles (a) corresponding to current density 10mA/cm² and (b) corresponding to current density 14mA/cm².

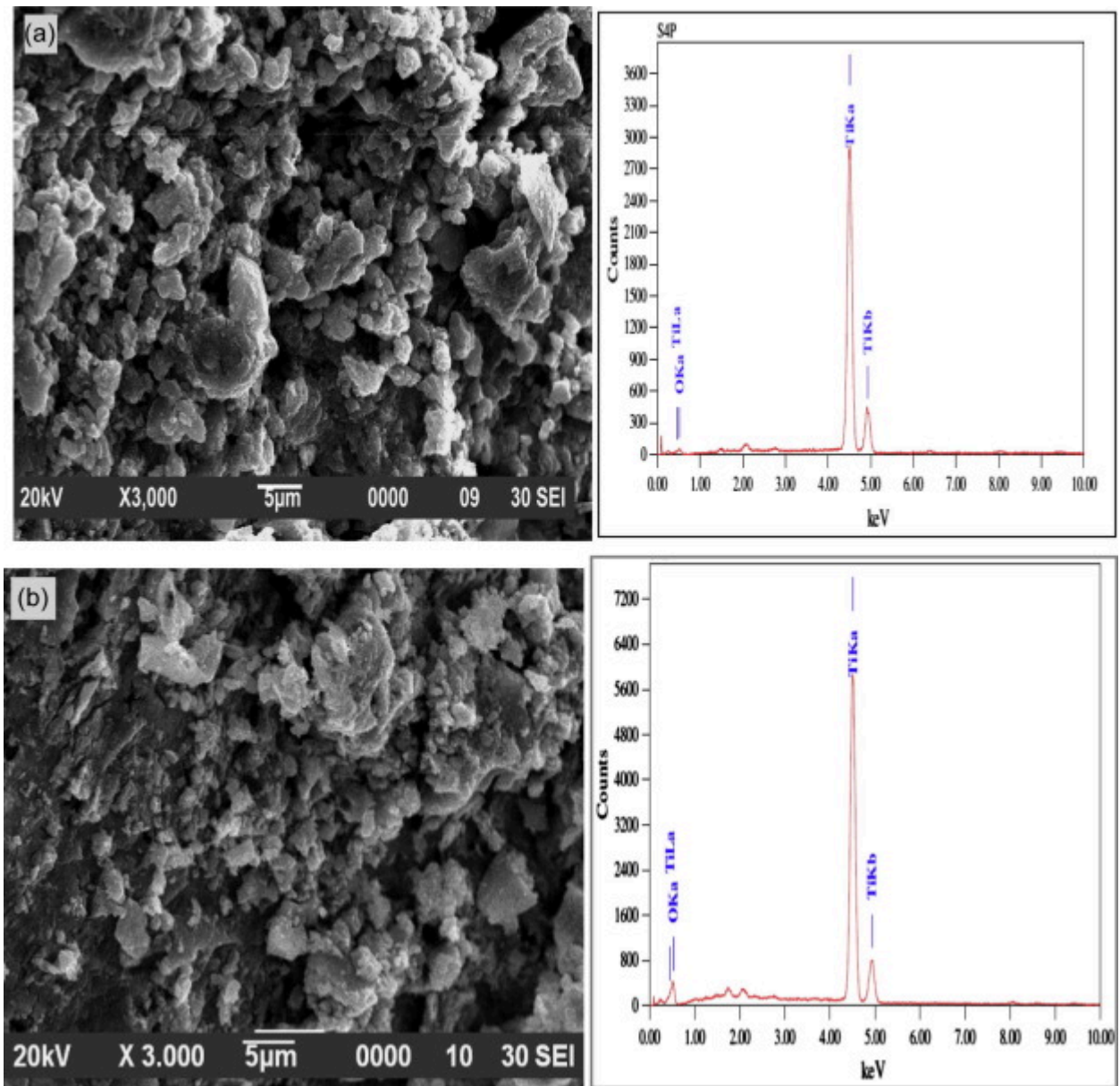
The average particle size calculated by using Debye–Scherrer Eq. (1) indicated high surface area.

$$d = \frac{K\lambda}{\beta \cos \theta} \quad (1)$$

where K known as Scherrer's constant (shape factor), ranging from 0.9 to 1.0, λ is the wavelength of the X-ray radiation source which is 1.54056, β is the width of the XRD peak at half height and θ is Bragg angle. XRD plot of TiO₂ nanoparticles synthesized at 10 and 14mA/cm² showed intense peak at (101) plane. The corresponding 2θ and FWHM values are 25.316° (0.3626°) and 25.306° (0.4392°) respectively and average crystalline size found to be 25 nm and 20 nm respectively.

3.3. SEM–EDS analysis

The SEM micrograph of TiO₂ nanoparticles synthesized at 10mA/cm² (Fig. 4a) and 14mA/cm² (Fig. 4b) showed there is dense agglomeration of particles and was irregular in shape. This was probably due to the partial solubility of the surfactant in the solvent under the given experimental conditions. TiO₂ nanoparticles synthesized with capping agent TPAB at both current densities were analyzed by EDS and are shown in Fig. 4a and b. The Ti and O peaks can be obviously found in both EDS spectra without any other peak like Br indicates that the pure TiO₂ particles are successfully prepared and there was complete removal of capping agent.



[Download : Download high-res image \(468KB\)](#)

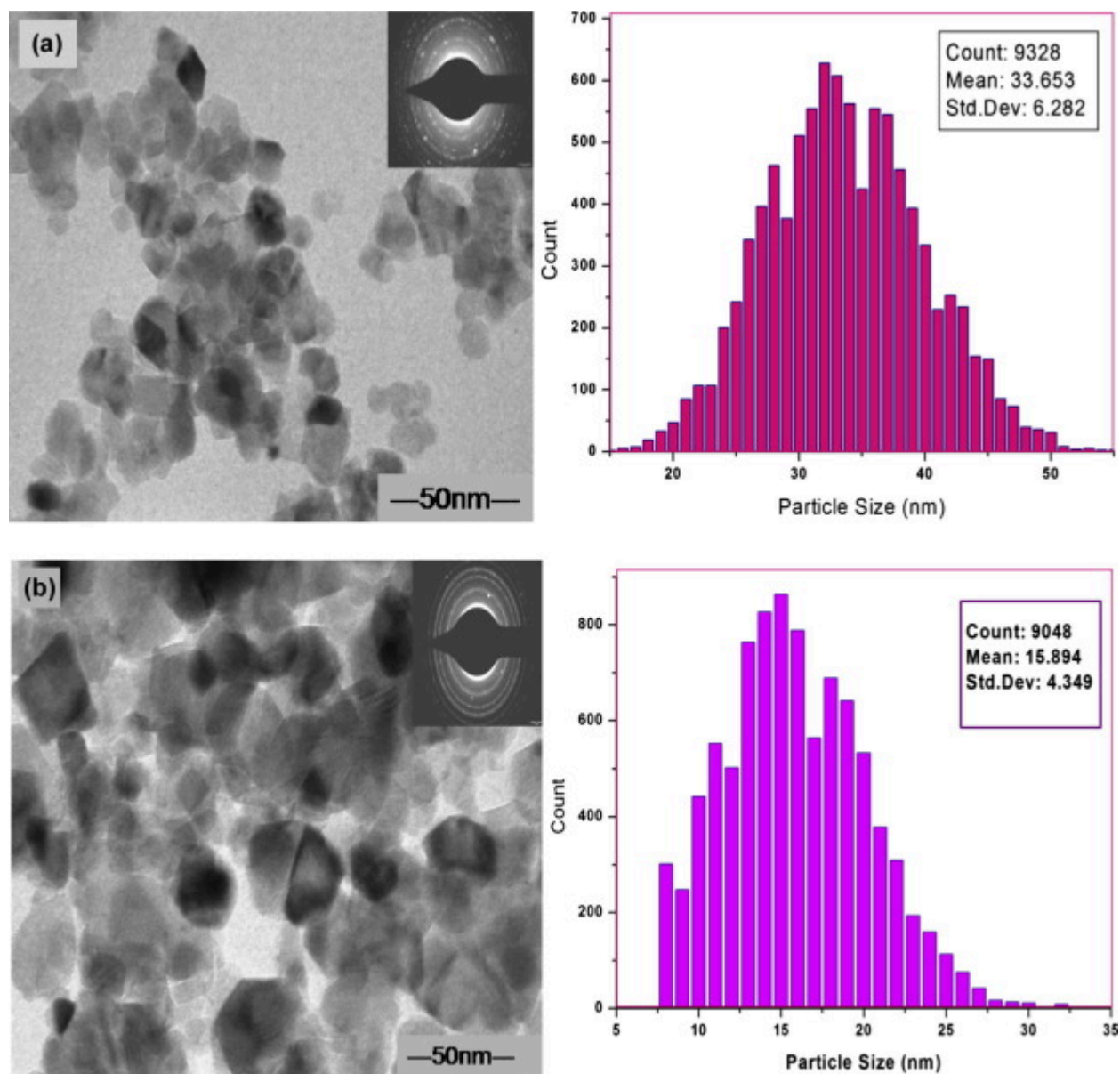
[Download : Download full-size image](#)

Figure 4. SEM image of TiO₂ nanoparticles. (a) Corresponding to current density 10mA/cm² with EDS spectrum and (b) corresponding to current density 14mA/cm² with EDS spectrum.

3.4. TEM analysis

The size, shape and phase composition of particles were studied by TEM. The sample for TEM analysis was obtained by evaporation of very dilute alcoholic suspensions onto carbon-coated copper grids. A TEM image (Fig. 5a and b) along with histogram of particle size distribution of the typical product showed that TiO₂ nanoparticles were dispersed and no aggregation was observed. The magnified image showed that these TiO₂ nanoparticles were entirely tetragonal in shape. The corresponding particle size distribution of TiO₂ nanoparticles was in agreement with the results calculated from the

XRD analysis. The electron diffraction studies indicated that TiO₂ nanoparticles were highly crystalline, as the pattern could be indexed to the anatase phase only (right inset of Fig. 5a and b). The *d* spacing calculated from the electron diffraction pattern matches the values obtained from XRD patterns. The crystalline nature of the electrochemically-synthesized TiO₂ nanoparticles is evident from the absence of the diffuse halo normally associated with the presence of amorphous phases.



[Download : Download high-res image \(326KB\)](#)

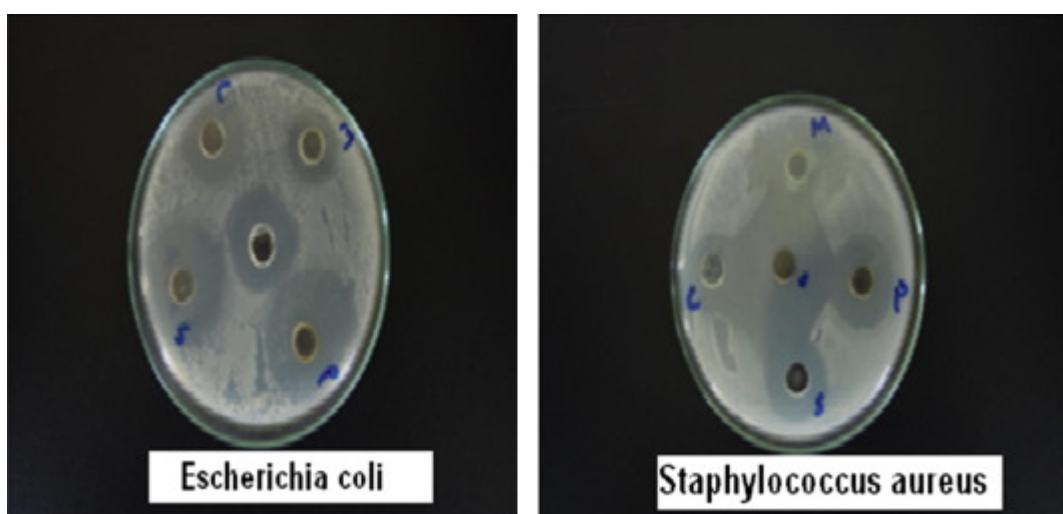
[Download : Download full-size image](#)

Figure 5. TEM images of TiO₂ nanoparticles at two different current densities. The upper right inset in (a) shows the related SAED pattern, and the lower right inset is an enlarged TEM image of TiO₂ nanoparticles prepared at 10 mA/cm² along with histogram on right side and in (b) upper right inset shows the related SAED pattern, and the lower right inset is an enlarged TEM image of TiO₂ nanoparticles prepared at 14 mA/cm² along with histogram.

3.5. Antibacterial activity study

According to several studies, it is believed that the metal oxides carry the positive charge while the microorganisms carry negative charges; this causes electromagnetic attraction between microorganisms and the metal oxides which leads to oxidization and finally death of microorganisms (Zhang and Chen, 2009). They cause pits or holes of bacterial cell wall could be associated with internalized particles, leading to increased permeability and cell death (Ravishankar and Jamuna, 2011, Holt and Bard, 2005). TiO₂ nanoparticles due to their small size and high surface to volume ratio undergo a higher level of interaction with the bacterial cells surface than the larger particles, resulting in a high antibacterial activity. It was observed that TiO₂ nanoparticles synthesized at two different current densities showed good antibacterial activity.

The antibacterial activity of TiO₂ nanoparticles (synthesized at two different current densities) was carried out by agar well diffusion method against *S. aureus* and *E. coli* for two different concentrations of TiO₂ nanoparticles 50µl and 100µl and gentamicin. The antibacterial circle photos of all samples are shown in Fig. 6. It is well known that if the diameter of antibacterial circle of one sample is larger than 7mm, it means that the sample has better antibacterial activity, however, if the diameter of antibacterial circle is equal to or less than 7mm, it means that the sample has poorer antibacterial activity. From the results in Table 1 it can be seen that all samples have better antibacterial activity because their antibacterial circle diameter is much larger than 7mm as well as the ACN/THF control did not show any antimicrobial activity against the tested bacterial strains. In addition, 100µl concentration of TiO₂ nanoparticles is better as compared to 50µl for inhibiting growth of bacterial test organism.



[Download](#) : [Download high-res image \(68KB\)](#)

[Download](#) : [Download full-size image](#)

Figure 6. Photographs of agar plate containing Gentamicin as standard antibiotics and different concentration of TiO₂ nanoparticles i.e. 50µl and 100µl of two different current

densities.

The TiO₂ nanoparticles proved to be very active on the tested Gram-positive strains, this differential sensitivity of Gram-negative and Gram-positive bacteria toward nanoparticles could be explained by the fact that the liquid medium is probably favoring the close interaction between the suspended nanoparticles and the Gram-positive microbial cells, which could better attach and anchor to the surface of the microbial cell, causing structural changes and damages leading to cell death (Chwalibog et al., 2012). The Gram-positive bacteria have a relatively thick wall composed of many layers of peptidoglycan polymer, and only one membrane (plasma membrane). The Gram-negative bacteria have only a thin layer of peptidoglycan and a more complex cell wall with two cell membranes, an outer membrane, and a plasma membrane. The addition of the outer membrane of the Gram-negative bacteria cells influences the permeability of many molecules. Under certain conditions, the Gram-negative bacteria are more resistant to many chemical agents than Gram-positive cells. In addition, the cell walls of Gram-negative bacteria are more prone to mechanical breakage because of the low amount of peptidoglycan (Tortora et al., 2001).

It appears that the antibacterial activity of the nanomaterials increased with increase in surface-to-volume ratio due to the decrease in size of nanoparticles. It is clear from the XRD and TEM results that TiO₂ nanoparticles synthesized at 14mA/cm² are smaller in size compared to TiO₂ nanoparticles synthesized at 10mA/cm². Table 1 shows TiO₂ nanoparticles synthesized at 14mA/cm² (15.99nm) nanoparticles exhibited maximum (19.1 mm) bacterial growth inhibition against *S. aureus* and (17.0mm) against *E. coli* in the form of zone-of-inhibition studies. In contrast, TiO₂ nanoparticles synthesized at 10mA/cm² showed zones of inhibition of 17.2mm against *S. aureus* and 14.3mm against *E. coli* respectively.

4. Conclusions

The efficiency of electrochemical method for the synthesis of titanium dioxide nanoparticles at two different current densities is demonstrated. The procedure offers several advantages including control of particles size, excellent yields, operational simplicity and minimum environmental effects. UV-Vis spectra showed an absorption band at 362nm and 346nm which is blueshifted compared to the bulk anatase TiO₂, indicating the formation of nanoparticles solution. From XRD analysis it is clear that particle size decreased with increase in current density as the current density is proportional to the rate of formation of Ti ion reduction to Ti adatoms. TEM and SEM analysis proved a nearly tetragonal morphology of particles. EDX analysis revealed the presence of Ti, O element without any other peak like Br indicates that the pure TiO₂ particles are successfully prepared and there was complete removal of capping agent.

The broadest range of antibacterial activity showed by TiO₂ nanoparticles against Gram-positive (*S. aureus*) and Gram-negative (*E. coli*) bacterial reference may be due to those particles' small size, large surface area and more active sites for carrying out catalytic reactions. Obtained results recommend the use of TiO₂ as effective antibacterial agent in practical application.

Acknowledgments

Department of Chemistry, Dr. Babasaheb Ambedkar Marathwada University, Aurangabad acknowledges the financial assistance of UGC-SAP-DRS-1 scheme New Delhi. One of the author (ASR) is thankful for financial assistance from UGC Major Research Project, New Delhi.

[Recommended articles](#)

References

[Akhavan, 2009](#) O. Akhavan

Lasting antibacterial activities of Ag–TiO₂/Ag/a-TiO₂ nanocomposite thin film photocatalysts under solar light irradiation

J. Colloid Interface Sci., 336 (2009), pp. 117-124, [10.1016/j.jcis.2009.03.018](https://doi.org/10.1016/j.jcis.2009.03.018) ↗

 [View PDF](#) [View article](#) [View in Scopus](#) ↗ [Google Scholar](#) ↗

[Baraton, 2011](#) M.-I. Baraton

Nano-TiO₂ for solar cells and photocatalytic water splitting: scientific and technological challenges for commercialization

Open Nanosci. J., 5 (2011), pp. 64-77

[CrossRef](#) ↗ [Google Scholar](#) ↗

[Bian et al., 2008](#) F. Bian, X.Z. Zhang, Z.H. Wang, Q. Wu, H. Hu, J.J. Xu

Preparation and size characterization of silver nanoparticles produced by femtosecond laser ablation in water

Chin. Phys. Lett., 25 (12) (2008), pp. 4463-4465

[View in Scopus](#) ↗ [Google Scholar](#) ↗

[Bumajdad et al., 2014](#) A. Bumajdad, M. Madkour, Y. Abdel-Moneam, M. El-Kemary

Nanostructured mesoporous Au/TiO₂ for photocatalytic degradation of a textile dye: the effect of size similarity of the deposited Au with that of TiO₂ pores

J. Mater. Sci., 49 (2014), pp. 1743-1754, [10.1007/s10853-013-7861-0](https://doi.org/10.1007/s10853-013-7861-0) ↗

[View in Scopus](#) [Google Scholar](#)

[Burda et al., 2000](#) C. Burda, T. Green, C. Landes, S. Link, R. Little, J. Petroski, M.A. El-Sayed

Optical spectroscopy of nanophase material

Z.L. Wang (Ed.), *Characterization of Nanophase Materials* (first ed.), Wang, Wiley-VCH, Weinheim (2000), pp. 197-241

[Google Scholar](#)

[Cheng et al., 2012](#) W. Cheng, Z. Dongmei, S. Ligu, W. Yanjie, D. Yuhong

Preparation and application of CdTe nanocrystals

Prog. Chem., 24 (07) (2012), pp. 1277-1293

[View in Scopus](#) [Google Scholar](#)

[Chong et al., 2010](#) M.N. Chong, B. Jina, W.K. Chowc Christopher, C. Saint

Recent developments in photocatalytic water treatment technology

Water Res., 44 (2010), pp. 2997-3027, [10.1016/j.watres.2010.02.039](https://doi.org/10.1016/j.watres.2010.02.039)

 [View PDF](#) [View article](#) [View in Scopus](#) [Google Scholar](#)

[Chwalibog et al., 2012](#) A. Chwalibog, E. Sawosw, A. Hotowy, J. Szeliga, K. Mitura, M. Grodzik, P. Orłowski, A. Sokolowska

Visualization of interaction between inorganic nanoparticles and bacteria or fungi

Int. J. Nanomed., 5 (2012), pp. 1085-1094, [10.2147/IJN.S13532](https://doi.org/10.2147/IJN.S13532)

[Google Scholar](#)

[Cooper et al., 2014](#) J.S. Cooper, M. Myers, E. Chow, L.J. Hubble, *et al.*

Performance of graphene, carbon nanotube, and gold nanoparticle chemiresistor sensors for the detection of petroleum hydrocarbons in water

J. Nanopart. Res., 16 (2014), p. 2173, [10.1007/s11051-013-2173-5](https://doi.org/10.1007/s11051-013-2173-5)

[View in Scopus](#) [Google Scholar](#)

[Foster et al., 2011](#) H.A. Foster, I.B. Ditta, S. Varghese, A. Steele

Photocatalytic disinfection using titanium dioxide: spectrum and mechanism of antimicrobial activity

Appl. Microbiol. Biotechnol., 90 (6) (2011), pp. 1847-1868, [10.1007/s00253-011-3213-7](https://doi.org/10.1007/s00253-011-3213-7)

[View in Scopus](#) [Google Scholar](#)

[Gajbhiye et al., 2009](#) M. Gajbhiye, J. Kesharwani, A. Ingle, A. Gade, M. Rai

Fungus-mediated synthesis of silver nanoparticles and their activity against pathogenic fungi in combination with fluconazole

Nanomed.–Nanotechnol., 5 (4) (2009), pp. 382-386, [10.1016/j.nano.2009.06.005](https://doi.org/10.1016/j.nano.2009.06.005) ↗

 [View PDF](#) [View article](#) [View in Scopus](#) ↗ [Google Scholar](#) ↗

[Holt and Bard, 2005](#) K.B. Holt, A.J. Bard

Interaction of silver (1) ions with the respiratory chain of *Escherichia coli*: an electrochemical and scanning electrochemical microscopy of micromolar Ag

Biochemistry, 44 (39) (2005), pp. 13214-13223

[CrossRef](#) ↗ [View in Scopus](#) ↗ [Google Scholar](#) ↗

[Kim et al., 2003](#) B. Kim, D. Kim, D. Cho, S. Cho

Bactericidal effect of TiO₂ photocatalyst on selected food-borne pathogenic bacteria

Chemosphere, 52 (1) (2003), pp. 277-281, [10.1016/S0045-6535\(03\)00051-1](https://doi.org/10.1016/S0045-6535(03)00051-1) ↗

 [View PDF](#) [View article](#) [View in Scopus](#) ↗ [Google Scholar](#) ↗

[Liou and Chang, 2012](#) J.W. Liou, H.H. Chang

Bactericidal effects and mechanisms of visible light-responsive titanium dioxide photocatalysts on pathogenic bacteria

Arch. Immunol. Ther. Exp., 60 (4) (2012), pp. 267-275, [10.1007/s00005-012-0178-x](https://doi.org/10.1007/s00005-012-0178-x) ↗

[View in Scopus](#) ↗ [Google Scholar](#) ↗

[Obida et al., 2005](#) M.Z. Obida, H.H. Afify, M.O. Abou-Helal, H.A.H. Zaid

Nanocrystalline anatase titania thin films synthesized by spray pyrolysis for gas detection

Egypt. J. Solids, 28 (1) (2005), pp. 35-51

[Google Scholar](#) ↗

[Porod et al., 2003](#) W. Porod, G. Csaba, A.I. Csurgay

A computing architecture composed of field-coupled single domain nanomagnets clocked by magnetic field

Int. J. Circuit Theory Appl., 31 (2003), pp. 67-82, [10.1002/cta.226](https://doi.org/10.1002/cta.226) ↗

[Google Scholar](#) ↗

[Ravishankar and Jamuna, 2011](#) R.V. Ravishankar, B.A. Jamuna

Nanoparticles and their potential application as antimicrobials

A. Méndez-Vilas (Ed.), Science Against Microbial Pathogens: Communicating Current Research and Technological Advances, Formatex, Badajoz (2011), pp. 197-209

[Google Scholar](#) ↗

[Reetz and Helbig, 1994](#) M.T. Reetz, W. Helbig

Size selective synthesis of nanostructure transition metal clusters

J. Am. Chem. Soc., 116 (1994), pp. 7401-7402

[CrossRef](#) [View in Scopus](#) [Google Scholar](#)

[Reetz et al., 1995](#) M.T. Reetz, W. Helbig, S.A. Quaiser

Electrochemical preparation of nanostructural bimetallic clusters

Chem. Mater., 7 (1995), pp. 2227-2228

[CrossRef](#) [View in Scopus](#) [Google Scholar](#)

[Rothenberg et al., 2002](#) G. Rothenberg, M.B. Thathagar, J. Beckers

Copper-catalyzed Suzuki cross-coupling using mixed nanocluster catalysts

J. Am. Chem. Soc., 124 (40) (2002), pp. 11858-11859, [10.1021/ja027716+](#)

[Google Scholar](#)

[Thornberry, 1950](#) H.H. Thornberry

A paper-disk plate method for the quantitative evaluation of fungicides and bactericides

Phytopathology, 40 (1950), pp. 419-429

[Google Scholar](#)

[Tian et al., 2013](#) W.C. Tian, Y.H. Ho, C.H. Chen, C.Y. Kuo

Sensing performance of precisely ordered TiO₂ nanowire gas sensors fabricated by electron-beam lithography

Sensors, 13 (2013), pp. 865-874, [10.3390/s130100865](#)

[View in Scopus](#) [Google Scholar](#)

[Tortora et al., 2001](#) G. Tortora, R.B. Funke, L.C. Case

Microbiology: An Introduction

Addison-Wesley Longman Inc., New York (2001)

[Google Scholar](#)

[Xie et al., 2011](#) Y. Xie, Y. He, P.L. Irwin, T. Jin, X. Shi

Antibacterial activity and mechanism of action of zinc oxide nanoparticles against campylobacter jejuni

Appl. Environ. Microbiol., 77 (7) (2011), pp. 2325-2331, [10.1128/AEM.02149](#)

[View in Scopus](#) [Google Scholar](#)

[Zhang and Chen, 2009](#) H. Zhang, G. Chen

Potent antibacterial activities of Ag/TiO₂ nanocomposite powders synthesized by a one-pot sol-gel method

Environ. Sci. Technol., 34 (8) (2009), pp. 2905-2910

[CrossRef](#) [View in Scopus](#) [Google Scholar](#)

Cited by (82)

Photocatalytic dye decomposition by bio-enzyme enriched TiO₂/g-C₃N₄ nanocomposite and assessment of toxicity of resultant water using *Catla catla* fish

2024, Biocatalysis and Agricultural Biotechnology

[Show abstract](#) 

Application of nanotechnology in the agricultural and food processing industries: A review

2024, Sustainable Materials and Technologies

[Show abstract](#) 

A critical review on the recent trends of photocatalytic, antibacterial, antioxidant and nanohybrid applications of anatase and rutile TiO₂ nanoparticles

2024, Science of the Total Environment

[Show abstract](#) 

Functional modification of TC4 by Cu-containing titanium dioxide films

2024, Ceramics International

[Show abstract](#) 

Zinc-based nanofertilizers: synthesis and toxicity assessments

2024, Nanofertilizer Synthesis: Methods and Types

[Show abstract](#) 

Sulfur and magnesium-based nanofertilizer: synthesis, characterization, and applications

2024, Nanofertilizer Synthesis: Methods and Types

[Show abstract](#) 



[View all citing articles on Scopus ↗](#)

Peer review under responsibility of King Saud University.

© 2019 Published by Elsevier B.V. on behalf of King Saud University.



All content on this site: Copyright © 2024 Elsevier B.V., its licensors, and contributors. All rights are reserved, including those for text and data mining, AI training, and similar technologies. For all open access content, the Creative Commons licensing terms apply.

